

UC Santa Barbara

UC Santa Barbara Previously Published Works

Title

Seebeck coefficient of a quantum confined, high-electron-density electron gas in SrTiO₃

Permalink

<https://escholarship.org/uc/item/5r0274d6>

Journal

Applied Physics Letters, 100(16)

Authors

Cain, Tyler

Lee, SungBin

Moetakef, Pouya

et al.

Publication Date

2012-04-16

Peer reviewed

Seebeck coefficient of a quantum confined, high-electron-density electron gas in SrTiO₃

Tyler A. Cain,¹ SungBin Lee,² Pouya Moetakef,¹ Leon Balents,² Susanne Stemmer,^{1,a)} and S. James Allen²

¹Materials Department, University of California, Santa Barbara, California 93106-5050, USA

²Department of Physics, University of California, Santa Barbara, California 93106-9530, USA

(Received 13 February 2012; accepted 31 March 2012; published online 16 April 2012)

We report on the Seebeck coefficient of quantum confined electron gases in GdTiO₃/SrTiO₃ heterostructures. These structures contain two-dimensional electron gases with very high sheet-carrier concentrations on the SrTiO₃-side of the interface due to intrinsic interface doping. While the sheet carrier concentrations are independent of the thickness of the SrTiO₃ layer, the Seebeck coefficient initially increases with SrTiO₃ thickness before saturating at a value of $\sim 300 \mu\text{K/V}$. A model of the Seebeck coefficient, based on thermally populated, self-consistent, tight binding subbands, captures in a semi-quantitative manner the observed thickness dependence.

© 2012 American Institute of Physics. [<http://dx.doi.org/10.1063/1.4704363>]

SrTiO₃-based materials are of great interest for thermoelectric applications, because of the high thermoelectric power factor ($S^2\sigma$, where S is the Seebeck coefficient and σ the electrical conductivity) of doped SrTiO₃, which is similar to that of the best commercial thermoelectrics.^{1–3} Similar to traditional thermoelectrics, for which quantum confinement has been investigated extensively as a means to enhance the Seebeck coefficient,^{4–8} reports in the literature indicate an enhanced Seebeck coefficient in SrTiO₃-based heterostructures.⁹ However, this apparent increase in the Seebeck coefficient was later attributed to artifacts from substrate conduction.¹⁰ Recent investigations of two-dimensional electron gases (2DEGs) at SrTiO₃/LaAlO₃ interfaces and in delta-doped SrTiO₃ layers have found no enhancement of the Seebeck coefficient compared to bulk.^{1,11} In addition to its potential for improving the thermoelectric properties, the Seebeck coefficient of 2DEGs in SrTiO₃ is also of scientific interest as it allows for unique insights into transport properties of 2DEGs in a prototype d -band material.

In this Letter, we investigate the Seebeck coefficient of high-density 2DEGs at epitaxial SrTiO₃/GdTiO₃ interfaces. At these interfaces, a 2DEG forms to compensate a fixed charge at the interface between the polar surface of (001) GdTiO₃ and the nonpolar surface of (001) SrTiO₃. The interfaces are characterized by a constant sheet carrier density of $\sim 3 \times 10^{14} \text{ cm}^{-2}$ per interface, even for very thin SrTiO₃ layers ($\sim 1 \text{ nm}$).¹² Because of a staggered band alignment, the high-density 2DEG resides largely in the wider band-gap SrTiO₃.¹² By inserting thin SrTiO₃ layers between two GdTiO₃ layers, quantum wells with sheet carrier densities as large as $6 \times 10^{14} \text{ cm}^{-2}$ can be obtained.

SrTiO₃/GdTiO₃ layers were grown by MBE on (001) (LaAlO₃)_{0.3}(Sr₂AlTaO₆)_{0.7} (LSAT) substrates, as described elsewhere.^{12,13} LSAT remains insulating, even under the very reducing conditions required for growth of GdTiO₃.¹³ Two types of high-electron-concentration samples grown by MBE are investigated here: GdTiO₃/SrTiO₃ on LSAT and GdTiO₃/

SrTiO₃/GdTiO₃ on LSAT, which has two electrically active interfaces. Ohmic contacts of 300 nm Au/50 nm Ti were deposited by electron beam evaporation. The Hall resistivity was measured using a physical properties measurement system (quantum design PPMS) in Van der Pauw and 6-contact Hall bar geometries. In-plane Seebeck coefficients were measured at room temperature using Peltier modules to generate a temperature gradient end-to-end across 1-cm-wide samples and type-K thermocouples were used to measure the resultant temperature difference (ΔT). The potential difference, ΔV , was measured by an Agilent 34401 A Digital Multimeter using voltage probes placed onto the Ohmic contacts, directly adjacent to the thermocouples. The Seebeck coefficient was calculated from a linear fit of ΔV versus ΔT . GdTiO₃ films grown directly on LSAT were insulating, i.e., showing an increase in resistance with decreasing temperature.¹² They showed a positive Seebeck coefficient of $24 \mu\text{V/K}$, which is smaller in magnitude than bulk GdTiO₃ (Ref. 14) and probably an indication of slight nonstoichiometry.¹⁵ Consistent with this, the resistivity of the GdTiO₃ films ($\sim 8 \Omega \text{ cm}$ at room temperature) was somewhat lower than that of bulk [$26 \Omega \text{ cm}$ (Ref. 16)]. More severely nonstoichiometric GdTiO₃ films would become metallic¹⁷ and show a reduced Curie temperature,¹⁸ neither of which was observed for the films investigated here (see Refs. 12 and 13). All heterostructures containing both SrTiO₃ and GdTiO₃ exhibited negative, n -type, Seebeck coefficients, due to the space charge layer at the interface, which consists of mobile electrons.

The Seebeck coefficients of GdTiO₃/SrTiO₃/LSAT structures (one conductive interface) are shown in Fig. 1 as a function of SrTiO₃ layer thickness. With increasing SrTiO₃ thickness, the Seebeck coefficient changes from $-60 \mu\text{V/K}$ for 0.4 nm thick SrTiO₃ to about $-300 \mu\text{V/K}$ for 130 nm thick SrTiO₃. In contrast, the sheet carrier density remains nearly independent of thickness, $\sim 3 \times 10^{14} \text{ cm}^{-2}$ (see Ref. 12 and also Fig. 2). As discussed elsewhere,¹² the sheet carrier density is a consequence of an electronic reconstruction of approximately $1/2$ electron per surface unit cell at each GdTiO₃/SrTiO₃ interface.

For comparison, the solid line in Fig. 1 shows the Seebeck coefficient of doped (or alloyed) bulk SrTiO₃, taken from Refs.

^{a)} Author to whom correspondence should be addressed. Electronic mail: stemmer@mrl.ucsb.edu.

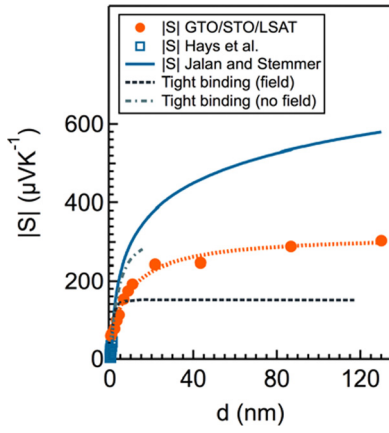


FIG. 1. Magnitude of the Seebeck coefficient (closed orange circles) for $\text{GdTiO}_3/\text{SrTiO}_3/\text{LSAT}$ heterostructures as a function of SrTiO_3 layer thickness d . All GdTiO_3 layers were 8 nm thick. The dotted orange line is a guide to the eye. The solid blue line and open squares are the magnitude of the Seebeck coefficient for uniformly La-doped SrTiO_3 films from Ref. 1 (Jalan and Stemmer) and of polycrystalline ($\text{Sr}_{1-x}\text{La}_x\text{TiO}_3$) samples from Ref. 19 (Hays *et al.*), respectively, where the Seebeck coefficients at each thickness are shown for a three-dimensional carrier concentration calculated as $n_{3D} = 3 \times 10^{14}/d[\text{cm}^{-3}]$. In extracting the data from Ref. 19, it was assumed that each La donates one electron to the conduction band, which is a reasonable assumption even for high La concentrations.²⁰ The dashed line is a tight binding calculation including quantum confinement and the self-consistent, spatially varying electric potential and the dashed-dotted line is the calculation for only film quantum confinement.

1 and 19, assuming that the constant sheet carrier density, $\sim 3 \times 10^{14} \text{ cm}^{-2}$, is distributed uniformly in the SrTiO_3 , producing a three-dimensional (3D) carrier concentration given by $n_{3D} = 3 \times 10^{14}/d[\text{cm}^{-3}]$, where d is the SrTiO_3 thickness for each sample. SrTiO_3 uniformly doped to a sheet carrier density of $\sim 3 \times 10^{14} \text{ cm}^{-2}$ at each thickness is expected to show a rapid and steady increase in Seebeck coefficient as the effective n_{3D} decreases. In contrast, the Seebeck coefficient of the $\text{GdTiO}_3/\text{SrTiO}_3/\text{LSAT}$ structures saturates for thicknesses above ~ 20 nm, with only a modest increase with thickness.

At the lowest thicknesses (≤ 1 nm), the magnitude of the Seebeck coefficient for the quantum confined structures is enhanced relative to the Seebeck coefficient of uniformly doped samples with the corresponding 3D carrier concentration [Figs. 2(a) and 2(b)]. At these thicknesses, the corresponding 3D carrier concentrations are extremely large—as high as 10^{22} cm^{-3} for the sample with two conductive $\text{GdTiO}_3/\text{SrTiO}_3$ interfaces that is shown in Fig. 2(b). To achieve such large carrier concentrations in bulk, almost 95% of the SrTiO_3 would have to be substituted with LaTiO_3 .²⁰ Such a system would be better described as Sr-doped LaTiO_3 and is near a cross-over from a negative to a positive Seebeck coefficient,¹⁹ and clearly very different from the interface-doped quantum wells studied here. For the $\text{GdTiO}_3/\text{SrTiO}_3$ heterostructures, the Seebeck coefficient of the samples with the thinnest SrTiO_3 layers asymptotically approaches a value that depends on the total 2-D density: the SrTiO_3 layer with larger electron density [two active interfaces, Fig. 2(b)] has an asymptotically smaller magnitude of the Seebeck coefficient.

To understand the thickness dependence of the Seebeck coefficient in Figs. 1 and 2, we consider two possible contributions: (1) a 2DEG that is bound to the interface by the interfacial positive charge and (2) a possible contribution

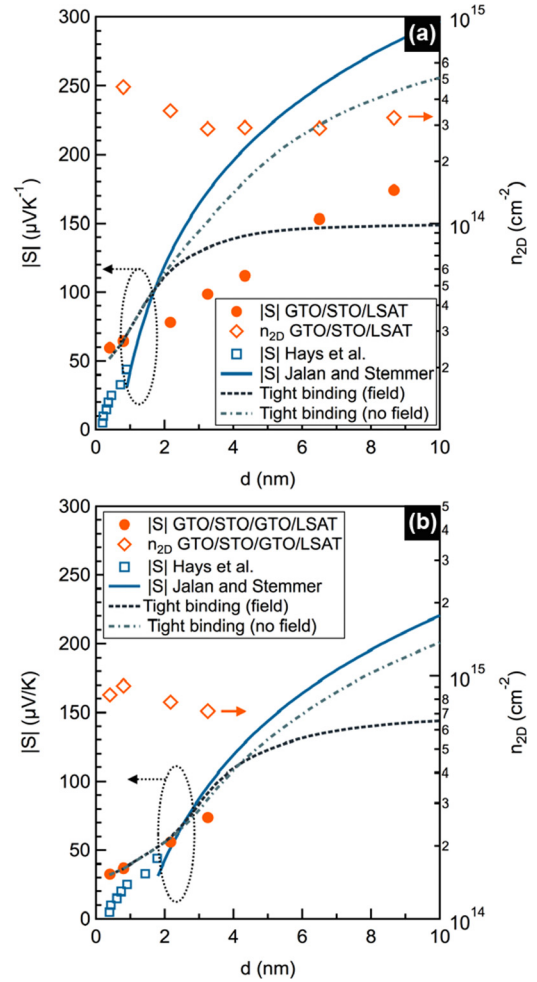


FIG. 2. (a) Same as Fig. 1, but showing only the data for the smaller SrTiO_3 thicknesses. (b) Magnitude of the Seebeck coefficient (closed circles) for $\text{GdTiO}_3/\text{SrTiO}_3/\text{GdTiO}_3/\text{LSAT}$ layers as a function of SrTiO_3 layer thickness. All GdTiO_3 layers were 4 nm thick. The solid blue line and open squares are literature values derived as described for Fig. 1. The measured two-dimensional carrier concentration is also shown (open orange diamonds). The dashed line is a tight binding calculation including quantum confinement and the self-consistent, spatially varying electric potential and the dashed-dotted line is the calculation for only film quantum confinement.

from residual uniform doping of the bulk of the SrTiO_3 , for example, due to oxygen vacancies.¹³ The contribution from the 2DEG to the Seebeck coefficient will become essentially constant when the thickness of the SrTiO_3 is larger than the spatial extent of the 2DEG. In contrast, any contributions from any background doping of the SrTiO_3 would increase with thickness until the transport becomes dominated by the bulk. The modest slope of the Seebeck coefficient versus thickness at large thickness may be a measure of the bulk contribution. Figure 1 shows that to approximately 20 nm, the contribution from the interface is significantly more important. The measured Seebeck coefficient (S_{measured}) of two parallel-connected layers maybe described by⁴

$$S_{\text{measured}} = \frac{S_{2D}n_{2D}\mu_{2D} + S_{\text{bulk}}(n_{\text{bulk}}d)\mu_{\text{bulk}}}{n_{2D}\mu_{2D} + (n_{\text{bulk}}d)\mu_{\text{bulk}}}, \quad (1)$$

where n_{2D} , $n_{\text{bulk}}d$ and μ_{2D} , μ_{bulk} are the respective sheet carrier concentrations and mobilities for the 2DEG and bulk components. For the layers in Fig. 1, the transport in the bulk is significantly less than that in the 2D space charge

($n_{2D}\mu_{2D} \gg (n_{bulk}d)\mu_{bulk}$) as the Hall effect determined sheet carrier density shows no appreciable dependence on thickness. We approximate Eq. (1) as

$$S_{measured} \approx S_{2D}(d) + S_{bulk} \frac{(n_{bulk}d)\mu_{bulk}}{n_{2D}\mu_{2D}}. \quad (2)$$

Under these conditions, Eq. (2) indicates that the contribution from the bulk is reduced by the ratio of the effective conductances and will increase linearly with thickness. A slow increase with thickness, observed in Fig. 1, could be caused by a bulk background doping of the order of 10^{18} cm^{-3} . At the largest thickness, this would add to the 2D carrier density measured by the Hall effect, but still constitute only a small fraction of the carrier densities shown in Fig. 2.

The contribution to the Seebeck coefficient from the high-density 2DEG, $S_{2D}(t)$, which is bound to the interface, can be calculated with a self-consistent, tight binding model (Hartree approximation) for the subbands that are thermally populated at room temperature.²¹ We assume electrons are in the t_{2g} orbitals dominated by π bonding: a single hopping parameter, t , is used to describe the electron transfer in the π bonded direction. We treat both film quantum confinement and confinement by the self-consistent, spatially varying electric potential produced by the mobile 2DEG and balanced by the fixed positive charge at the $\text{GdTiO}_3/\text{SrTiO}_3$ interface (dashed lines in Figs. 1 and 2). For comparison, model calculations that ignore the self-consistent potential and only includes film quantum confinement by assuming an arbitrarily large dielectric constant or that the effective charge on the carriers is zero are also shown (dashed-dotted lines). As shown in Figs. 1 and 2, these models provide insight into the SrTiO_3 thickness dependence of the Seebeck coefficient. In particular, for the thinnest SrTiO_3 , the model quantitatively agrees with the experiment for both types of heterostructures and carrier concentrations. Within the models, transport is controlled by film quantum confinement for thicknesses below 3 nm, or ~ 8 unit cells. Only at larger thicknesses does the confinement by the electrostatic forces begin to play an important role (see differences between dashed and dashed-dotted lines).

For sufficiently large quantum well thicknesses, the 2DEG should not experience the film thickness quantum confinement and only the self-consistent potential binding of the 2DEG to the positive charge at the interface will be operative. The Seebeck coefficient will then plateau when the thickness exceeds the width of the 2DEG. This is qualitatively seen in both experiments and model calculations (Fig. 1). However, the model calculation, assuming a SrTiO_3 dielectric constant of $277 \epsilon_0$, plateaus at a substantially lower value for the Seebeck coefficient and at a smaller thickness. This hard saturation and plateau is imposed by the finite spatial extent of the electrostatically confined space charge. The continued increase with thickness and soft saturation of the Seebeck coefficient seen in the experiment indicates that the spatial extent of the space charge is $\sim 2-3$ times larger than predicted by the self consistent tight binding model used here. Therefore, the self consistent, tight binding model for the thermally populated electric subbands binds the space charge layer too strongly to the interface.

In summary, Seebeck measurements of $\text{GdTiO}_3/\text{SrTiO}_3$ heterostructures provide evidence that the carriers do not

uniformly spread out across the layers, but form a confined 2DEG at the interface. A tight binding model quantitatively explains the magnitude and thickness dependence in the extreme quantum limit, that is, for SrTiO_3 quantum wells that are less than ~ 3 nm wide. In this limit, quantum confinement is dictated by the film thickness and the effects of the spatially varying electric potential appear to be less important. For thick SrTiO_3 layers, the Seebeck coefficient is determined by a 2DEG electrostatically bound to the interface. A self-consistent tight binding model produces a 2DEG that is too tightly bound to the interface. The latter points to the need for more sophisticated treatments of the self-consistent potential, such as non-linear screening in SrTiO_3 or corrections to the Hartree approximation.

T.A.C., P.M., and S.S. acknowledge support through the Center for Energy Efficient Materials, an Energy Frontier Research Center funded by the DOE (Award Number DE-SC0001009). T.A.C. was supported by the Department of Defense through a NDSEG fellowship. S.J.A. acknowledges funding through the UCSB MRL, which is supported by the MRSEC Program of the NSF under Award No. DMR-1121053. S.B.L. and L.B. acknowledge support by the Army Research Office through a MURI program (Grant No. W911-NF-09-1-0398). The work made use of the UCSB Nanofabrication Facility, a part of the NSF-funded NNIN network.

¹B. Jalan and S. Stemmer, *Appl. Phys. Lett.* **97**, 042106 (2010).

²T. Okuda, K. Nakanishi, S. Miyasaka, and Y. Tokura, *Phys. Rev. B* **63**, 113104 (2001).

³H. P. R. Frederikse, W. R. Thurber, and W. R. Hosler, *Phys. Rev.* **134**, A442 (1964).

⁴P. Pichanusakorn and P. Bandaru, *Mater. Sci. Eng. R* **67**, 19 (2010).

⁵L. D. Hicks and M. S. Dresselhaus, *Phys. Rev. B* **47**, 12727 (1993).

⁶L. D. Hicks, T. C. Harman, and M. S. Dresselhaus, *Appl. Phys. Lett.* **63**, 3230 (1993).

⁷C. J. Vineis, A. Shakouri, A. Majumdar, and M. G. Kanatzidis, *Adv. Mater.* **22**, 3970 (2010).

⁸D. A. Broido and T. L. Reinecke, *Appl. Phys. Lett.* **77**, 705 (2000).

⁹H. Ohta, S. Kim, Y. Mune, T. Mizoguchi, K. Nomura, S. Ohta, T. Nomura, Y. Nakanishi, Y. Ikuhara, M. Hirano, H. Hosono, and K. Koumoto, *Nature Mater.* **6**, 129 (2007).

¹⁰M. L. Scullin, C. Yu, M. Huijben, S. Mukerjee, J. Seidel, Q. Zhan, J. Moore, A. Majumdar, and R. Ramesh, *Appl. Phys. Lett.* **92**, 202113 (2008).

¹¹I. Pallecchi, M. Codda, E. G. d'Agliano, D. Marre, A. D. Caviglia, N. Reyren, S. Gariglio, and J. M. Triscone, *Phys. Rev. B* **81**, 085414 (2010).

¹²P. Moetakef, T. A. Cain, D. G. Ouellette, J. Y. Zhang, D. O. Klenov, A. Janotti, C. G. V. d. Walle, S. Rajan, S. J. Allen, and S. Stemmer, *Appl. Phys. Lett.* **99**, 232116 (2011).

¹³P. Moetakef, J. Y. Zhang, A. Kozhanov, B. Jalan, R. Seshadri, S. J. Allen, and S. Stemmer, *Appl. Phys. Lett.* **98**, 112110 (2011).

¹⁴G. V. Bazuev and G. P. Shveikin, *Izv. Akad. Nauk. SSSR, Neorg. Mater.* **14**, 267 (1978).

¹⁵H. D. Zhou and J. B. Goodenough, *Phys. Rev. B* **71**, 165119 (2005).

¹⁶M. Reedyk, D. A. Crandles, M. Cardona, J. D. Garrett, and J. E. Greedan, *Phys. Rev. B* **55**, 1442 (1997).

¹⁷M. Heinrich, H. A. K. von Nidda, V. Fritsch, and A. Loidl, *Phys. Rev. B* **63**, 193103 (2001).

¹⁸A. C. Komarek, H. Roth, M. Cwik, W. D. Stein, J. Baier, M. Kriener, F. Bouree, T. Lorenz, and M. Braden, *Phys. Rev. B* **75**, 224402 (2007).

¹⁹C. C. Hays, J.-S. Zhou, J. T. Markert, and J. B. Goodenough, *Phys. Rev. B* **60**, 10367 (1999).

²⁰Y. Tokura, Y. Taguchi, Y. Okada, Y. Fujishima, T. Arima, K. Kumagai, and Y. Iye, *Phys. Rev. Lett.* **70**, 2126 (1993).

²¹N. W. Ashcroft and N. D. Mermin, *Solid State Physics* (Brooks/Cole, Belmont, 1976).